Aceh Int. J. Sci. Technol., 10(1) 27-37
April 2021
doi: 10.13170/aijst.10.1.18890

Aceh International Journal of Science and Technology
ISSN: p-2088-9860; e-2503-2398
Journal homepage: http://jurnal.unsyiah.ac.id/aijst

Bentonite and Magnetite Filler-Modified Polyurethane Foam in Fixed Bed Column for the Adsorption of Mercury (II) Ions from Aqueous Solution

Siti Sarah[1], Adisalamun[1], Darmadi[1], Suraiya Kamaruzzaman[1], Abrar Muslim[1*], Saiful[2]
[1]Department of Chemical Engineering, Faculty of Engineering, Universitas Syiah Kuala, Indonesia
[2]Department of Chemistry, Faculty of Mathematics and Science, Universitas Syiah Kuala, Indonesia
*Corresponding author: *abrar.muslim@che.unsyiah.ac.id*

Received : December 2, 2020
Accepted : April 5, 2021
Online : April 30, 2021

Abstract – This paper proposed adsorbent development by synthesizing polyurethane foam (PUF) using a simple method, mixing polyol with isocyanate and adding fillers of bentonite and magnetite to the PUF matrix. The study's main objective was to produce a PUF-based adsorbent with high reactivity to remove Hg^{2+} in wastewater. This bentonite and magnetite filler-modified polyurethane foam (BMPUF) adsorbent was fixed in a bed column for the adsorption of mercury (II) ions from an aqueous solution. The effect of initial Hg^{2+} concentration on the removal rate and the effect of contact time on adsorption efficiency was investigated. Langmuir, Freundlich, and BET non-linear models were taken into account to determine the best adsorption isotherm fitting and obtain adsorption capacity, intensity, and pore volume. As a result, it followed the non-linear Freundlich model, and the average adsorption capacity and intensity were 0.466 mg/g and 0.923, respectively. The average BET-based pore volume obtained was 0.782 L/mg. The kinetics study showed that the non-linear pseudo-first-order kinetics model was more suitable for describing the Hg2+ adsorption kinetics. The maximum equilibrium adsorption capacity was 1.770 mg/g with the adsorption rate of 0.0013 min^{-1} based on the non-linear model. The effect of varying bentonite and magnetite ratio on adsorption isotherm and kinetics was also investigated. Overall, the potential application of BMPUF adsorbent in the adsorption of mercury (II) ions was demonstrated in the current study.

Keywords: Adsorption, bentonite, magnetite, mercury (II) ions, polyurethane foam.

Introduction

Adsorption is one of the well-known and favorable separation processes due to many advantages. It offers low operating costs, ease of operation, simple design, environmentally friendly, and high effectiveness. Various adsorbents are available, making it one of the most widely used methods for treating water polluted by hazardous contaminants, especially mercury (II) ions (Vali *et al.*, 2018).

Uncountable research attempts have been progressing continuously in developing new materials as appropriate and effective adsorbents for mercury remediation from wastewater (Ali *et al.*, 2018; Chen *et al.*, 2018; Huang *et al.*, 2019). The adsorbent material desired for the adsorption process must have large porosity, high surface area, and abundant active sites for adsorbate to be adsorbed (Gusain *et al.*, 2019; Kumar Fosso-Kankeu *et al.*, 2019).

Besides the excellent characteristics and outstanding separation performance, other properties such as reusability, generation method, and stability should also be highly considered in developing a new adsorbent material (Ke *et al.*, 2017; Abraham *et al.*, 2018). So far, the majority of the adsorbents used for heavy metals removal are in powder form; hence their application is complicated and expensive due to the difficulty in separating the adsorbent from batch mode solution. In addition, the small particle size of the adsorbent is not very suitable for application in column system adsorption (Ramana *et al.*, 2010; Luo *et al.*, 2015). Therefore, various fixed bed materials have been recently proposed to solve the problems addressed in the previous studies

(Malkoc and Nuhoglu, 2006). To support the particles of adsorbent, polyurethane foam (PUF) which has a high ratio of surface area to mass and highly porous structure, can be utilized in a fixed bed column (Vali *et al.*, 2018).

PUF is a polymer that can absorb various chemical substances because it has both polar and non-polar groups. Free molecules, dithionate metals, aromatic compounds, and complex anions can be separated using PUF (Hong *et al.*, 2018). Potential organic and inorganic fillers can be added to the PUF matrix to improve the adsorption capacity, efficiency, and selectivity of environmental remediation. This organic and inorganic filler-modified PUF allows the adsorbent to interact with pollutants without restrictions, and it can be separated easily from contaminated water (Mahfoudhi and Boufi, 2017). Nanocarbon filler-modified PUF in the walled tube was successfully applied for adsorption of safranin T and P (II) (Khan *et al.*, 2015). Cellulose acetate-based PUF modified has been effectively used to adsorb Cr (VI) ions in solution (Riaz *et al.*, 2016).

This study proposed the development of bentonite and magnetite filler-modified polyurethane foam (BMPUF) adsorbent. Bentonite was chosen as a filler not only because it is abundant in nature and affordable, but it is also well known for having excellent adsorption ability, especially against heavy metal ions in liquid systems (Allo and Murray, 2004). In comparison, magnetite was selected for its magnetic trait to increase the reactivity of the adsorbent against the Hg^{2+} ions (Fawzia *et al.,* 2020). BMPUF adsorbent was fixed in a bed column for the adsorption of mercury (II) ions from an aqueous solution. The effect of initial Hg^{2+} concentration and contact time on the performance of BMPUF adsorbent was investigated. Adsorption isotherm study was completed using Langmuir, Freundlich, and BET non-linear models to determine the best fitting and obtain the value of related parameters. The non-linear pseudo-first-order and pseudo-second-order of the adsorption kinetics model were taken into account to get the best fit and value of the associated parameters. The effect of bentonite and magnetite ratio in the BMPUF adsorbent on adsorption isotherm and kinetics was also investigated.

Materials and Methods

Materials involved in synthesizing the BMPUF adsorbents were magnetite (Fe_3O_4, Merck), bentonite (non-commercial), polyol (Merck), isocyanate (Merck), Hg standard solution (1000 ppm, Merck), and distilled water.

Preparation of bentonite includes grinding the bentonite into a powder form with a uniform particle size of 80-100 mesh. Following that, bentonite was physically activated by calcination process at 400 ° C for 4 hours.

The synthesis of BMPUF adsorbent was initiated by mixing polyol and isocyanate with a volume ratio of 1:1 and stirring until homogeneous. Bentonite added with magnetite in the mass ratio of 2% and 5% was poured into the mixing polyol and isocyanate solution, then mixed for a few minutes until it was thoroughly mixed. The resulting mixture was immediately poured into the molds and then rested until it solidified. Solid BMPUF was then reshaped into a tubular form with a diameter and height of 2 cm.

Adsorption experiment

Standard solution of Hg^{2+} at 1000 mg/L was diluted into various concentrations of 1, 2, and 3 mg/L then placed in a fixed column reactor with a volume of 250 ml each. After that, BMPUF adsorbent was added, and the process was set with a contact time of 240 min with stirring at 110 rpm. Once finished, 5 ml of each sample filtrate was pipette, and its concentration was determined by using atomic absorption spectrometry (AAS, Analyst 800 Perkin Elmer Co, Norwaik CT USA) analysis.

The adsorption efficiency is the percentage of Hg^{2+} metal ions adsorbed by BMPUF 2% and BMPUF 5% adsorbents at contact times of 0, 40, 80, 120, 160, and 240 minutes. Equation (1) was used to determine the efficiency of adsorption (Delgado *et al.* 2019):

$$\eta = \frac{(C_0 - C_e)}{C_0} 100\% \quad (1)$$

where η (%) represents the efficiency of adsorption, C_0 is adsorbate initial concentration in aqueous solution before adsorption (mg/L), and Ce is the adsorbate concentration after adsorption at a specific contact time (mg/L).

The adsorption capacity of Hg using polyurethane bentonite magnetite for each adsorption time can be expressed by using Equation (2) (Muslim *et al.*, 2016; Ramadhani *et al.*, 2021):

$$q_{t=n} = \frac{(C_{t=0} - C_t)V_S}{m_{AC}} \quad (2)$$

where $C_{t=0}$ represents adsorbate concentration in aqueous solution at the time of zero (t = 0 min), C_t denotes as the adsorbate concentration in aqueous solution at a certain time (t (min)), $q_{t=n}$ (mg/g) indicates the adsorption capacity at the certain time, Vs (L) is the volume of the solution when taking a sample at the certain time, and m_{AC} represents the adsorbent mass.

Adsorption Isotherms

The study of adsorption isotherms was done using three isotherm models: non-linear Langmuir, Freundlich, and BET models. The standard model of Langmuir equations in nonlinear form is generally represented as (Muslim *et al.*, 2016):

$$q_e = \frac{Q_0 b C_e}{1 + bC_e} \quad (3)$$

The linearized form is expressed as follows:

$$\frac{C_{eq}}{Q_{eq}} = \frac{1}{K_L Q_{\max}} + \frac{C_{eq}}{Q_{\max}} \quad (4)$$

C_{eq} is the equilibrium concentration of the adsorbate (mg/L), and q_e is the amount of adsorbate adsorbed per unit mass of adsorbent at equilibrium (mg/g). $Q_{\max}$ is the maximum amount of substance adsorbed per unit weight of adsorbent to form an entire layer, and K_L is a constant related to the location of the binding site. Plot C_{eq}/Q_{eq} vs. C_{eq} will produce a straight line that is a slope $1/Q_{\max}$ and intercept $1/K_L.Q_{\max}$ (Foo and Hameed 2010).

For the Freundlich isotherm model, the equations used are in nonlinear (Eq. 5) and linear (Eq. 6) forms and the parameters can be obtained when the log q_e is plotted vs. log C_e, which produces a straight line with $1/n$ as the slope and log (K_F) as the intercept (Muslim, *et al.* 2016).

$$q_e = K_F C_e^{-1/n} \quad (5$$

$$\log q_e = \frac{1}{n}\log C_e + \log K_F \quad (6)$$

K_F (mg/g) is the relative adsorption capacity of the adsorbent, and n is the Freundlich constant obtained by plotting log q_e vs. log C_e. The type of this isotherm is indicated by the value of n, where the parameters K_F and n are temperature dependent. $1/n$ is the adsorption intensity or surface heterogeneity, showing the relative energy distribution and heterogeneity of the adsorbed site (Al-Ghouti and Da'ana, 2020).

The linear equation form of the BET model is expressed as follows (Foo and Hameed, 2010):

$$\frac{C_e}{q_e(C_s - C_e)} = \frac{1}{q_s C_{BET}} + \frac{(C_{BET} - 1)}{q_s C_{BET}}\left(\frac{C_e}{C_s}\right) \quad (7)$$

From a linear plot $\frac{C_e}{q_e(C_s - C_e)}$ vs $\frac{C_e}{C_s}$, C_{BET} and q_s can be calculated from the slope and the intercept. Because C_{BET} and $C_{BET}(C_e/C_s)$ has a value greater than 1, this equation can be simplified into:

$$q_e = \frac{q_s}{1 - \left(\frac{C_e}{C_s}\right)} \quad (8$$

This model is extended to the liquid-solid interface and is described in nonlinear form as follows:

$$q_e = \frac{q_s C_{BET} C_e}{(C_s - C_e)\left[1 + (C_{BET} - 1)\left(\frac{C_e}{C_s}\right)\right]} \quad (9)$$

Adsorption kinetics

The determination of the adsorption kinetics was carried out using two methods, namely the Pseudo-order one, the second-order pseudo-model (Malekbala *et al.* 2015, Muslim *et al.* 2015). The first pseudo-order model is expressed by Equations 10 and 11:

$$\ln(q_e - q_t) = \ln q_e - k_1 t \quad (10)$$

where k_1 is the pseudo-first-order reaction rate constant determined by plotting $\ln(q_e\text{-}q_t)$ vs. *t*.

The pseudo-second-order model is expressed by the Equation (Muslim *et al.*, 2017):

$$\frac{t}{q_t} = \frac{1}{k_2 q_e^{\,2}} + \frac{t}{q_e} \quad (11)$$

where k_2 is the pseudo-second-order reaction rate constant, determined from the intercept and slope from plotting t/q_t vs. *t*.

Results

Effect of initial concentration on the rate of adsorption

In this research, the prepared BMPUF adsorbents with two different loadings were tested for their performance in adsorbing Hg^{2+} from artificial mercury contaminants of several varied concentrations, namely 1, 2, and 3 mg/L. The removal rate of the Hg^{2+} by BMPUF adsorbents can be seen in Figure 1.

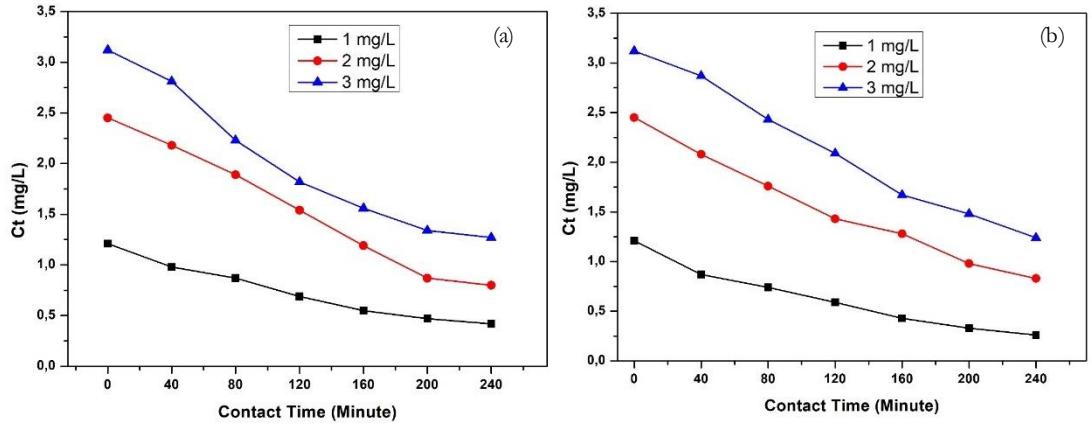

Figure 1. T The effect of the initial concentration of the solution on the adsorption rate of Hg^{2+} metal using adsorbents (a) BMPUF 2%, and (b) BMPUF 5%.

Effect of contact time on adsorption efficiency

Figure 2 shows that the adsorption efficiency tended to increase with the length of contact time. Adsorption efficiency rose sharply in the first 120 min. As can also be observed in Figures 2a and 2b, experiments using Hg solution with an initial concentration of 3 mg/L showed the lowest efficiency gain compared to data from experiments at the other two initial concentrations.

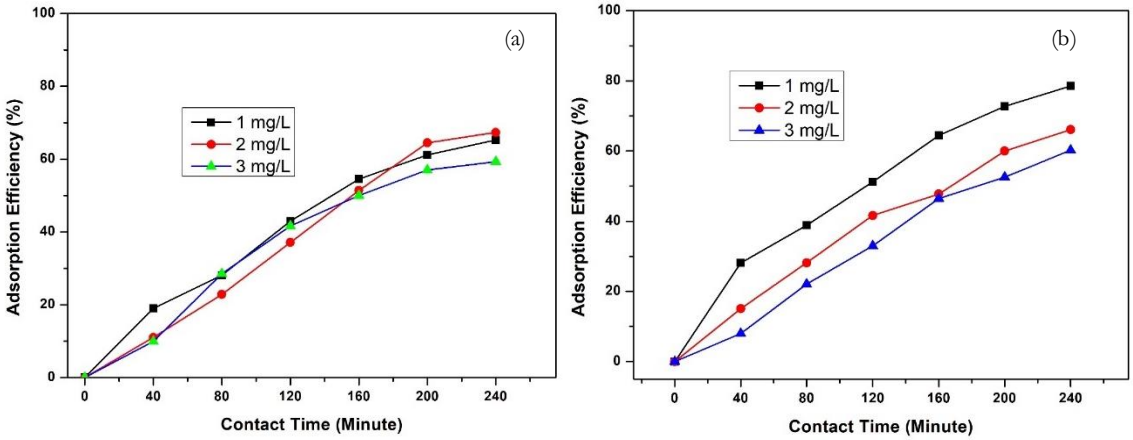

Figure 2. Effect of contact time on the efficiency of adsorption of Hg^{2+} metal using (a) BMPUF 2% and (b) BMPUF 5% adsorbents.

Adsorption isotherm

Adsorption equilibrium is important information showing the distribution of adsorbate molecules in the liquid and solid phases when the adsorption process reaches equilibrium. The adsorption isotherms analyzed in this study were Langmuir, Freundlich, and BET isotherms. The fitting Hg^{2+} adsorption isotherm model for 2% BMPUF and 5% BMPUF adsorbent was obtained from the *qe* vs. *Ce* plot. The non-linear graph for the three isotherm models above can be seen in Figures 3a and 3b.

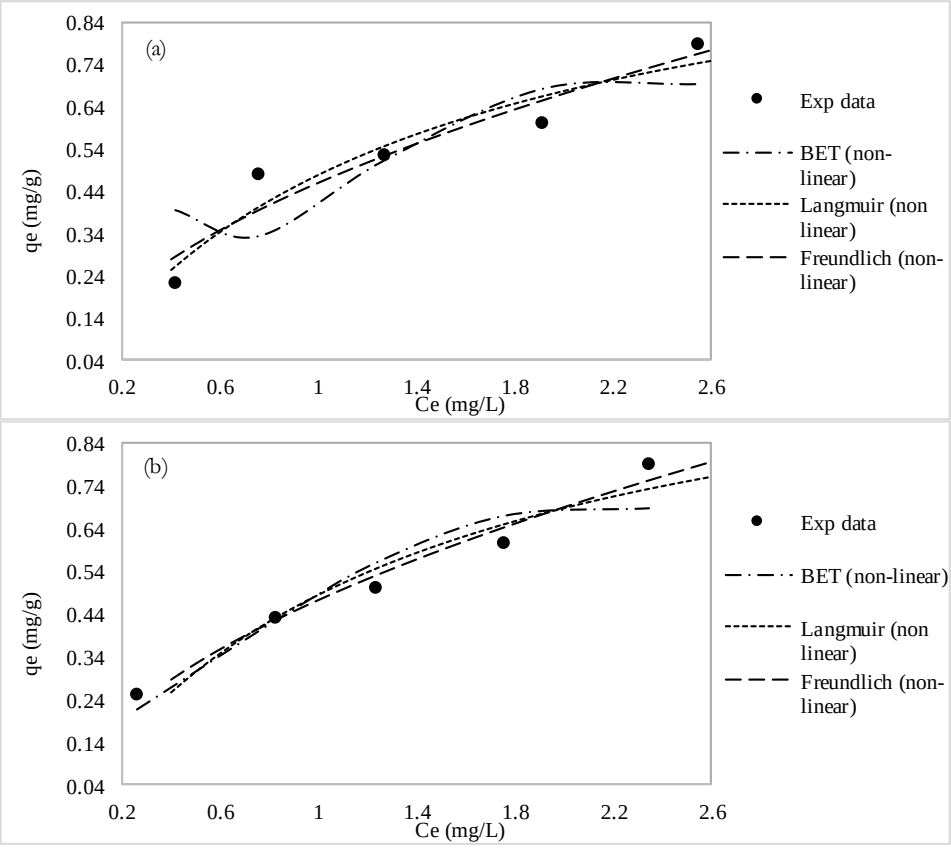

Figure 3. The non-linear isotherm model of the Hg^{2+} adsorption process using the (a) BMPUF 2% and (b) BMPUF 5% adsorbents.

Furthermore, to estimate isotherm parameters from non-linear equations, further optimization was needed using the add-in solver tool on Microsoft® Excel because non-linear equations were intrinsically more difficult to solve than linear equations. To determine which isotherm model fits each adsorbent, a non-linear analysis method by minimizing the non-linear value of the sum of squared errors (SSE) was used. From Table 1, it can be seen that the resulting isotherm constants (K_L, a_L, Q_o, K_f, n, q_s, and C_{BET}) obtained from the optimization procedure.

Table 1. Results of optimized adsorption isotherm models (non-linear).

Ads	Langmuir				Freundlich			BET		
	K_L (L/g)	a_L (L/mg)	Q_o (K_L/a_L)	SSE	K_f (mg/g)	n	SSE	q_s	C_{BET} (L/mg)	SSE
BMPUF 2%	0.8241	0.7152	1.2209	0.01402	0.4611	1.8451	0.00463	0.8002	0.8923	0.06675
BMPUF 5%	0.8252	0.7012	1.1768	0.01252	0.4712	1.8361	0.00437	1.1034	0.6723	0.01942

Table 2. Results of adsorption kinetics data.

Adsorbent	Co (mg/L)	Parameter	Pseudo-first order		Pseudo-second order	
			linear	*non-linear*	*linear*	*non-linear*
BMPUF 2%	**1**	qe_{exp} (mg/g)	0.2107	0.2107	0.2107	0.2107
		qe_{cal} (mg/g)	0.2689	0.3620	0.2687	0.4972
		k (min^{-1})	0.0134	0.0033	0.0301	0.0064
		SSE	-	0.0017	-	0.0002
		R^2	0.9378	0.9956	0.7359	0.9967
	2	qe_{exp} (mg/g)	0.5077	0.5077	0.5077	0.5077
		qe_{cal} (mg/g)	0.7784	1.7606	0.9130	2.8585
		k (min^{-1})	0.0143	0.0011	0.0048	0.0002
		SSE	-	0.0016	-	0.0017
		R^2	0.8242	0.9946	0.3073	0.9946
	3	qe_{exp} (mg/g)	0.5285	0.5285	0.5285	0.5285
		qe_{cal} (mg/g)	0.7655	0.8153	0.8683	2.0778
		k (min^{-1})	0.0157	0.0046	0.0069	0.0008
		SSE	-	0.0039	-	0.0025
		R^2	0.9168	0.9932	0.4121	0.9890
BMPUF 5%	**1**	qe_{exp} (mg/g)	0.2452	0.2452	0.2452	0.2452
		qe_{cal} (mg/g)	0.2839	0.3043	0.2856	0.4506
		k (min^{-1})	0.0123	0.0067	0.0544	0.0109
		SSE	-	0.0003	-	0.000295
		R^2	0.9495	0.9962	0.8418	0.9968
	2	qe_{exp} (mg/g)	0.3857	0.3857	0.3857	0.3857
		qe_{cal} (mg/g)	0.4658	0.6840	0.5117	1.1550
		k (min^{-1})	0.0110	0.0034	0.0171	0.0018
		SSE	-	0.0003	-	0.0003
		R^2	0.9204	0.9986	0.645	0.9986
	3	qe_{exp} (mg/g)	0.470	0.470	0.470	0.470
		qe_{cal} (mg/g)	1.7015	1.7703	0.9294	2.7685
		k (min^{-1})	0.0104	0.0013	0.0038	0.0003
		SSE	-	0.0016	-	0.0016
		R^2	0.9472	0.9962	0.2149	0.9963

The non-linear method was used to determine the isotherm model because this method was more suitable for isothermal equilibrium studies. It has the advantage in which the error distribution cannot be changed as easily as that of the linear method (Vilardi *et al.* 2018, Vilela *et al.*, 2019). In this process, the SSE acts as a minimized objective function value to produce the best isothermic constant parameters by minimizing the difference between experimental and theoretical data predicted by non-linear isotherm models (Karri *et al.*, 2017).

Adsorption kinetics

Adsorption kinetics states the rate of adsorption rate or rate that occurs in the adsorption process. To determine the kinetics rate and mechanism of the adsorption of Hg^{2+} on the adsorbent, Lagergren's Pseudo-first order, and Ho's pseudo-second-order rate equations were used. To find a more suitable model of these two equations, regression analysis was carried out based on linear and non-linear methods. The linear method is analyzed based on the suitability of the Equation with experimental data. In contrast, the non-linear method was analyzed based on the data optimization process, which offered a very flexible conformance function curve, minimizing the error value. The kinetics parameters from the adsorption process using BMPUF 2% and BMPUF 5% adsorbents are shown in Table 2.

As seen in Table 2, there are several parameters such as pseudo-first-order rate constant (k_1), pseudo-second-order rate constant (k_2), theoretical adsorption capacity (qe_{alc}), and the regression coefficient (R^2) in the linear method which obtained from the slope and intercept of the *ln (qe-qt)* vs. t plot, and the t/qt vs. t plot. Meanwhile, the parameters in the non-linear method were obtained through a solver add-in on Microsoft® Excel, with the principle of minimizing SSE and optimizing the value of the regression coefficient (R^2).

Discussion

Effect of initial concentration on the rate of adsorption

Figure 1 shows that the solution concentration (C_t) decreases from the initial concentration with the increasing of the contact time, indicating that the adsorption rate of Hg^{2+} increased with prolonged time. In the first 160 min, the adsorption rate showed a good increasing trend but tended to be constant after extended contact time. This result was due to the reduced availability of the active adsorbent site. Active sites are the adsorptive part of the chemical functional groups; every active site is capable of binding at least or maximum one molecule of Hg^{2+}, the Hg^{2+} molecule is bonded on the active site of the adsorbent through physical and chemical interaction. As the adsorption process is ongoing, most active sites will be occupied by the Hg2+ molecules, causing a decrease in Hg^{2+} that can be adsorbed onto the adsorbent (Chaukura *et al.*, 2017).

Figure 1 also shows that the initial concentration affected the Hg^{2+} removal rate. As can be observed, at the high initial concentration, the driving force for mass transfer was more significant and tended to remove obstacles to the mass transfer process; this phenomenon caused the removal rate to get better because the Hg^{2+} ions in the adsorbate solution were more easily transferred to the adsorption sites on the surface of the adsorbent (Ebrahimian Pirbazari *et al.* 2014).

Effect of contact time on adsorption efficiency

Adsorption efficiency increased sharply in the first 120 min was reasonable due to the presence of large numbers of active sites on the adsorbent surface, which were still free and have not been accommodated by Hg^{2+} metal ions (Martini *et al.* 2018). The lowest efficiency for the initial Hg^{2+} concentration of 3 mg/L compared to data from experiments at the other two initial concentrations was reasonable because, at a concentration of 3 mg/L, the solution contains a high amount of Hg and resulted in the adsorbent saturated and causes a decrease in adsorption due to the rapid formation of second, third, fourth layers and so on, or multilayer adsorption symptoms occurred which resulted in the adsorbent surface being saturated or almost saturated by the adsorbate (Malekbala *et al.* 2015).

Adsorption isotherm

The highest monolayer maximum capacity (Q_o) of the Langmuir isotherm model was obtained from the BMPUF 2% adsorbent, namely 1.2209 mg/g. This value was still considered low if compared to obtained Q_o from several other reports in which they obtained more than 30 mg/g (Şahan *et al.*, 2018). Meanwhile, the value of Langmuir constants (K_L and a_L) was observed to have insignificant differences either for BMPUF adsorbent

with a concentration of 2% or 5%, which are 0.82 and 0.70 L/g, respectively. This finding was not too different from those reported in previous research (Guerra *et al.* 2012, Park *et al.* 2018).

For the maximum adsorbent capacity (K_f) data from the Freundlich isotherm model, the two BMPUF adsorbents also showed somewhat comparable data, namely 0.46 and 0.47 mg/g BMPUF 2% and BMPUF 5%, respectively. The maximum adsorbent capacity obtained was still low under 1 mg/g because the initial concentration of Hg^{2+} in the solution was set at low in the range of 1-3 mg/L. A similar trend was also seen for the value of constant *n*; the results obtained in the experiment using BMPUF 2% and BMPUF 5% were not much different, namely 1.8451 and 1.8361, respectively. The *n* constant generally indicated the strength of the binding energy between the adsorbate and the adsorbent during the adsorption process (Yu, 2015). The *n* constant can be used to observe the isothermic nature; if $n > 1$, the adsorption process was favorable. Thus, it can be concluded that the adsorption process using both types of adsorbents in this study was favorable according to Freundlich isotherm fitting (Ebrahimian Pirbazari *et al.* 2014).

The optimized results of the BET isotherm model, which was shown in Table 1, illustrated the CBET values for BMPUF 2% and BMPUF 5% were 0.8923 L/mg and 0.6723 L/mg, respectively. Although the BMPUF 2% adsorbent had a CBET constant that was slightly higher than the BMPUF 5%, however, the constant value obtained for both adsorbents was still relatively low. It was reported that the CBET value <10 indicated that the interaction between the adsorbate ions on the adsorbent surface was weak, so the adsorbate ions tend to have high mobility and unstable (Lapham and Lapham 2019).

Determining the best isotherm model for each adsorbent can be done by observing the smallest SSE value of the three models. Therefore, from the optimized results in Table 1, the BMPUF 2% and BMPUF 5% adsorbents followed the Freundlich adsorption isotherm model. Freundlich's adsorption isotherm assumes that the adsorption occurs physically, meaning that more adsorption occurs on the surface of the adsorbent. In physical adsorption, the adsorbate is not firmly attached to the adsorbent surface. The adsorbate can move from one part of the adsorbate surface to another, and the surface that is left behind can be occupied by another moiety of the adsorbate. This physical adsorption occurs due to the Van Der Waals bonding, a weak attractive force between the adsorbate and the adsorbent surface (Malekbala *et al.*, 2015).

Adsorption kinetics

The data contained in Table 2 was used to determine which kinetics model fits the adsorption process in this study best by comparing the regression coefficient (R^2) between linear and non-linear models (Delgado *et al.*, 2019). Based on Table 2, it can be seen that the R^2 values from the non-linear method ($R^2 > 0.99$) were higher than those of the linear method. This showed that the non-linear adsorption kinetics model was more suitable to describe the Hg^{2+} kinetics of adsorption using BMPUF 2% and BMPUF 5% adsorbents.

As can be observed, the two adsorbents showed an insignificant difference in SSE value for it to be used as a determinant. However, it was seen that the theoretical adsorption capacity value ($q_{e\,cal}$) obtained from the pseudo-first-order kinetics model is closer to that of experimental adsorption capacity ($q_{e\,exp}$). Hence, it can be concluded that the adsorption process using BMPUF adsorbent both at 2% and 5% followed the pseudo-first-order kinetics model. The pseudo-first-order kinetic model indicated that the adsorption rate was directly proportional to the availability of free active sites on the adsorbent surface. The adsorption rate also depended on the amount of adsorbate on the adsorbent surface, as evidenced by the adsorption driving force (q_e-q_t), which is directly proportional to the number of active sites, the more the available free active sites, the higher the adsorption driving force (Tran *et al.* 2017).

Conclusion

The development of polyurethane-based adsorbent through the addition of bentonite and magnetite as the fillers has been done. The resulting adsorbent showcased the potential to be used as an adsorbent for mercury (II) removal with a decent removal rate and performance efficiency. The results of isotherms study by using three isotherm models, namely Langmuir, Freundlich, and BET. It was found, Freundlich model was the best fit, with the average adsorption capacity being 0.466 mg/g and intensity was being 0.923. The average BET-based pore volume obtained was 0.782 L/mg. The non-linear pseudo-first-order adsorption kinetics model was more suitable for describing the Hg2+ adsorption kinetics. The non-linear model-based maximum equilibrium

adsorption capacity obtained was 1.770 mg/g with the adsorption rate of 0.0013 min^{-1}. Overall, physical adsorption might contribute to Hg^{2+} adsorption on the BMPUF adsorbent.

Acknowledgment

The authors would like to thank the Chemical Engineering Department, especially the Chemical Process Laboratory, Unit Operation of Chemical Engineering Laboratory, and Process Instrumentation Laboratory at the Faculty of Engineering, Universitas Syiah Kuala, for technical support. The authors would like to express our deep appreciation for the Chemistry Laboratory Faculty of Mathematics and Science, Universitas Syiah Kuala, for the AAS analysis.

References

Abraham, A.M., Kumar, S.V., and Alhassan, S.M. 2018. Porous sulphur copolymer for gas-phase mercury removal and thermal insulation. Chemical Engineering Journal, 332: 1-7.

Al-Ghouti, M.A, and Da'ana, D.A. 2020. Guidelines for the use and interpretation of adsorption isotherm models: a review. Journal of Hazardous Materials, 393: 122383.

Ali, J., Wang, H. Ifthikar, J. Khan, A. Wang, T. Zhan, K. Shahzad, A. Chen, Z. and Chen, Z. 2018. Efficient, stable and selective adsorption of heavy metals by thio-functionalized layered double hydroxide in diverse types of water. Chemical Engineering Journal, 332: 387-397.

Allo, W.A., and Murray, H.H. 2004. Mineralogy, chemistry and potential applications of a white bentonite in San Juan province, Argentina. Applied Clay Science, 25: 237-243.

Chaukura, N., Murimba, E.C. and Gwenzi, W. 2017. Sorptive removal of methylene blue from simulated wastewater using biochars derived from pulp and paper sludge. Environmental Technology & Innovation, 8: 132-140.

Chen, J., Wang, Y. Wei, X. Xu, P. Xu, W. Ni, R. and Meng, J. 2018. Magnetic solid-phase extraction for the removal of mercury from water with ternary hydrosulphonyl-based deep eutectic solvent modified magnetic graphene oxide. Talanta, 188: 454-462.

Delgado, N., Capparelli, A. Navarro, A. and Marino, D. 2019. Pharmaceutical emerging pollutants removal from water using powdered activated carbon: Study of kinetics and adsorption equilibrium. Journal of Environmental Management, 236: 301-308.

Ebrahimian P.A., Saberikhah, E. Badrouh, M. and Emami, M. S. 2014. Alkali treated Foumanat tea waste as an efficient adsorbent for methylene blue adsorption from aqueous solution. Water Resources and Industry, 6: 64-80.

Fawzia, I.E., Dalia, E.M. and Omnia, A.A.E. 2020. Study the adsorption properties of magnetite nanoparticles in the presence of different synthesized surfactants for heavy metal ions removal. Egyptian Journal of Petroleum, 29: 1-7.

Foo, K.Y., and Hameed, B.H. 2010. Insights into the modeling of adsorption isotherm systems. Chemical Engineering Journal, 156: 2-10.

Guerra, D. L., Oliveira, S. P. Silva, R.A.S. Silva, E. M. and Batista, A.C. 2012. Dielectric properties of organofunctionalized kaolinite clay and application in adsorption mercury cation. Ceramics International, 38: 1687-1696.

Gusain, R., Kumar, N. Fosso-Kankeu, E. and Ray, S. S. 2019. Efficient Removal of Pb(II) and Cd(II) from Industrial Mine Water by a Hierarchical MoS2/SH-MWCNT Nanocomposite. ACS Omega, 4: 13922-13935.

Hong, H. J., Lim, J. S. Hwang, J. Y. Kim, M. Jeong, H. S. and Park, M. S. 2018. Carboxymethlyated cellulose nanofibrils (CMCNFs) embedded in polyurethane foam as a modular adsorbent of heavy metal ions. Carbohydrate Polymers, 195: 136-142.

Huang, Y., Xia, S. Lyu, J. and Tang, J. 2019. Highly efficient removal of aqueous Hg^{2+} and CH_3Hg^+ by selective modification of biochar with 3-mercaptopropyltrimethoxysilane. Chemical Engineering Journal, 360: 1646-1655.

Karri, R. R., Sahu, J. N. and Jayakumar, N. S. 2017. Optimal isotherm parameters for phenol adsorption from aqueous solutions onto coconut shell based activated carbon: Error analysis of linear and non-linear methods. Journal of the Taiwan Institute of Chemical Engineers, 80: 472-487.

Ke, F., Jiang, J. Li, Y. Liang, J. Wan, X. and Ko, S. 2017. Highly selective removal of Hg^{2+} and Pb^{2+} by thiol-functionalized Fe3O4@metal-organic framework core-shell magnetic microspheres. Applied Surface Science, 413: 266-274.

Khan, T.A., Nazir, M. Khan, E.A. and Riaz, U. 2015. Multiwalled carbon nanotube–polyurethane (MWCNT/PU) composite adsorbent for safranin T and Pb (II) removal from aqueous solution: Batch and fixed-bed studies. Journal of Molecular Liquids, 212: 467-479.

Kumar, N., Fosso-Kankeu, E. and Ray, S. S. 2019. Achieving Controllable MoS2 Nanostructures with Increased Interlayer Spacing for Efficient Removal of Pb (II) from Aquatic Systems. ACS Applied Materials & Interfaces, 11: 19141-19155.

Lapham, D. P., and Lapham, J. L. 2019. Gas adsorption on commercial magnesium stearate: The origin of atypical isotherms and BET transform data. Powder Technology, 342: 676-689.

Luo, X., Zeng, J. Liu, S. and Zhang, L. 2015. An effective and recyclable adsorbent for the removal of heavy metal ions from aqueous system: Magnetic chitosan/cellulose microspheres. Bioresource Technology, 194: 403-406.

Mahfoudhi, N., Boufi, S. 2017. Nanocellulose as a novel nanostructured adsorbent for environmental remediation: a review. Cellulose, 24: 1171-1197.

Malekbala, M.R., Khan, M.A. Hosseini, S. Abdullah, L.C. and Choong, T.S.Y. 2015. Adsorption/desorption of cationic dye on surfactant modified mesoporous carbon coated monolith: Equilibrium, kinetic and thermodynamic studies. Journal of Industrial and Engineering Chemistry, 21: 369-377.

Malkoc, E., and Nuhoglu, Y. 2006. Removal of Ni (II) ions from aqueous solutions using waste of tea factory: Adsorption on a fixed-bed column. Journal of Hazardous Materials, 135: 328-336.

Martini, B.K., Daniel, T.G. Corazza, M.Z. and De Carvalho, A.E. 2018. Methyl orange and tartrazine yellow adsorption on activated carbon prepared from boiler residue: Kinetics, isotherms, thermodynamics studies and material characterization. Journal of Environmental Chemical Engineering, 6: 6669-6679.

Muslim, A., Ellysa, E. and Said, S. D. 2017. Cu (II) ions adsorption using activated carbon prepared from *Pithecellobium jiringa* (Jengkol) shells with ultrasonic assistance: isotherm, kinetic and thermodynamic studies. Journal of Engineering & Technological Science, 49: 472-490.

Muslim, A., Husin, S. Ramli, S. Irfan, A. and Firdaus, F. 2016. Adsorption of Pb(II) in aqueous solutions by activated carbon prepared from empty fruit bunch of oil palm. The 7th International Conference on Green Technology, Malang, 5-6 October 2016, Malang, Faculty of Science and Technology, Maulana Malik Ibrahim State Islamic University. 2301-4490.

Muslim, A., Zulfian, I. M. Devrina, E. and Fahmi, H. 2015. Adsorption of Cu (II) from the aqueous solution by chemical activated adsorbent of areca catechu shell. Journal of Engineering Science Technology, 10: 1654-1666.

Park, J. H., Wang, J. J. Xiao, R. Pensky, S. M. Kongchum, M. Delaune, R. D. and Seo, D. C. 2018. Mercury adsorption in the Mississippi River deltaic plain freshwater marsh soil of Louisiana Gulf coastal wetlands. Chemosphere, 195: 455-462.

Ramana, D.K.V., Jamuna, K. Satyanarayana, B. Venkateswarlu, B. Rao, M.M. and Seshaiah, K. 2010. Removal of heavy metals from aqueous solutions using activated carbon prepared from Cicer arietinum. Toxicological & Environmental Chemistry, 92: 1447-1460.

Ramadhani, T., Abdullah, F. Indra, I. Muslim, A. Suhendrayatna, S. Meilina, H. and Saiful, S. 2021. Adsorption of Cd(II) ions from aqueous solution by a low-cost biosorbent prepared from ipomea pes-caprae stem. Aceh International Journal of Science and Technology, 9: 197-206.

Riaz, T., Ahmad, A. Saleemi, S. Adrees, M. Jamshed, F. Hai, A.M. and Jamil, T. 2016. Synthesis and characterization of polyurethane-cellulose acetate blend membrane for chromium (VI) removal. Carbohydrate Polymers, 153: 582-591.

Şahan, T., Erol, F. and Yılmaz, Ş. 2018. Mercury (II) adsorption by a novel adsorbent mercapto-modified bentonite using ICP-OES and use of response surface methodology for optimization. Microchemical Journal, 138: 360-368.

Tran, H.N., You, S.-J. Hosseini-Bandegharaei, A. and Chao, H. P. 2017. Mistakes and inconsistencies regarding adsorption of contaminants from aqueous solutions: a critical review. Water Research, 120: 88-116.

Vali, S.A., Baghdadi, M. and Abdoli, M.A. 2018. Immobilization of polyaniline nanoparticles on the polyurethane foam derived from waste materials: A porous reactive fixed-bed medium for removal of mercury from contaminated waters. Journal of Environmental Chemical Engineering, 6: 6612-6622.

Vilardi, G., Mpouras, T. Dermatas, D. Verdone, N. Polyder, A. A. and Di Palma, L. 2018. Nanomaterials application for heavy metals recovery from polluted water: The combination of nano zero-valent iron and carbon nanotubes. Competitive adsorption non-linear modeling. Chemosphere, 201: 716-729.

Vilela, P. B., Matias, C. A. Dalalibera, A. Becegato, V. A. and Paulino, A. T. 2019. Polyacrylic acid-based and chitosan-based hydrogels for adsorption of cadmium: Equilibrium isotherm, kinetic and thermodynamic studies. Journal of Environmental Chemical Engineering, 7: 103327.

Yu, W. 2015. Developments in modeling and optimization of production in unconventional oil and gas reservoirs. Dissertation. The University of Texas at Austin